

Electronic Supplementary Information (ESI) for

**Ionic Liquids Introduced into Supramolecular Isomeric Open-Frameworks
as Photocatalyst for Visible-Light-Driven Degradation of Organic Dyes**

Wen-Juan Ji ^{a,b}, Man-Cheng Hu^a, Shu-Ni Li^a, Yu-Cheng Jiang^a, Quan-Guo Zhai^{*a}

^a Key Laboratory of Macromolecular Science of Shaanxi Province,

School of Chemistry & Chemical Engineering,

Shaanxi Normal University, Xi'an, Shaanxi, 710062, P. R. China.

Tel: +86-29-81530767; E-mail: zhaiqg@snnu.edu.cn

^b School of Chemistry & Material Science,

Shanxi Normal University, Linfen, 041004,

Shanxi Province, P. R. China.

Materials and Methods

All reagents of A. R. grade employed were commercially available and used without further

purification. The FT-IR spectra (KBr pellets) were recorded on a Nicolet Avatar 360 FT-IR Spectrometer in the range of 4000–400 cm^{-1} . C, H, and N elemental analyses were determined on an Elementar Vario EL III elemental analyzer. Thermal stability studies were carried out on a NETSCHZ STA-449 C thermoanalyzer under air atmosphere (40–800 $^{\circ}\text{C}$ range) at a heating rate of 5 $^{\circ}\text{C min}^{-1}$.

Powder X-ray diffraction (PXRD) pattern was measured on a Rigaku DMAX 2500 powder diffractometer at 40 kV and 100 mA using Cu-K α ($\lambda = 1.54056 \text{ \AA}$), with a scan speed of 0.2 s/step and a step size of 0.02 $^{\circ}$. The simulated powder pattern was calculated using single-crystal X-ray diffraction data and processed by the free Mercury 2.3 program provided by the Cambridge Crystallographic Data Centre.

The solid-state and solution fluorescence spectra were measured at room temperature using a Cary Eclipse fluorescence spectrophotometer. The excitation slit and emission slit both were 2.5 nm. The UV-vis spectrum was recorded at room temperature on computer-controlled PE Lambda 900 UV-vis spectrometer equipped with an integrating sphere in the wavelength range 200–1600 nm. A BaSO $_4$ plate was used as a reference, on which finely ground powder of the sample was coated. The absorption spectrum was calculated from reflection spectra by the Kubelka-Munk function: $\alpha/S = (1-R)^2/2R$, where α is the absorption coefficient, S is the scattering coefficient that is practically wavelength independent when the particle size is larger than 5 μm , and R is the reflectance. The band gap value was determined as the intersection point between the energy axis at the absorption offset and the line extrapolated from the linear portion of the absorption edge in the α/S versus E (eV) plot.

The photo-reactor was designed with an internal light source (300 W high pressure mercury lamp for UV light irradiation and 300 W high pressure xenon lamp for visible-light irradiation) surrounding by a water-cooling quartz jacket to cool the lamp, where a 100 mL 0.05 mmol/L organic dye solution with the presence of solid catalyst (20 mg) were put in. The solution was stirred in the dark for 60 min to obtain a good dispersion and reach adsorption-desorption equilibrium between the organic molecules and the catalyst surface. At given intervals of illumination, 3 mL samples of the reaction solution were taken out and centrifuged to remove the photocatalyst particles. Then, the filtrates were analyzed by recording variations of the absorption band maximum in the UV-vis spectra of dyes by using a UV-1800 spectrometer.

Table S1. Crystal data and structure refinements for **1** and **2** (squeeze).

Compound	1	2
----------	----------	----------

Empirical formula	C ₃₄ H ₃₀ N ₄ O ₁₆ Zn ₃	C ₃₆ H ₃₄ N ₄ O ₁₆ Zn ₃
Formula weight	946.73	974.78
Crystal system	Orthorhombic	Orthorhombic
Space group	<i>Pnma</i>	<i>Fddd</i>
<i>a</i> (Å)	14.2823(19)	19.7430(3)
<i>b</i> (Å)	17.776(3)	26.8524(5)
<i>c</i> (Å)	27.245(3)	29.2175(5)
α (deg)	90	90
β (deg)	90	90
γ (deg)	90	90
<i>V</i> (Å ³)	6917.2(16)	15489.6(5)
<i>Z</i>	8	16
<i>F</i> (000)	3840	7936
ρ (mg/m ³)	1.818	1.672
Absorption coefficient (mm ⁻¹)	2.150	1.923
θ for data collection (deg)	3.07 to 25.01	3.26 to 26.37
Limiting indices	-16 \leq h \leq 16, -21 \leq k \leq 21, -28 \leq l \leq 32	-11 \leq h \leq 24, -24 \leq k \leq 33, -36 \leq l \leq 32
Reflections collected / unique	60831 / 6292	10043 / 3955
Unique reflections (R(int))	0.0459	0.0192
Parameters	380	186
Goodness-of-fit on <i>F</i> ²	1.067	1.014
<i>R</i> ₁ ^a , <i>wR</i> ₂ [<i>I</i> > 2 δ (<i>I</i>)]	0.0486, 0.1424	0.0291, 0.1070
<i>R</i> ₁ , <i>wR</i> ₂ (all data)	0.0528, 0.1461	0.0315, 0.1083
Largest diff. peak and hole (e \cdot Å ⁻³)	0.850, -0.454	0.459, -0.433

$$^a R_1 = \sum(|F_o| - |F_c|) / \sum|F_o|, wR_2 = [\sum w(F_o^2 - F_c^2)^2 / \sum w(F_o^2)^2]^{0.5}.$$

Table S2. Atomic coordinates ($\times 10^4$) and equivalent isotropic displacement parameters ($\text{\AA}^2 \times 10^3$) for **1** and **2**.

atom	x	y	z	U(eq)
			1	
Zn(1)	670(1)	242(1)	7982(1)	22(1)
Zn(2)	2442(1)	316(1)	6561(1)	20(1)
Zn(3)	1276(1)	-405(1)	5539(1)	35(1)
C(1)	1924(3)	1121(2)	7473(2)	24(1)
C(2)	3958(3)	1093(2)	7129(2)	22(1)
C(3)	2070(4)	2500	7472(2)	26(1)
C(4)	2496(3)	1812(2)	7382(2)	22(1)
C(5)	3430(3)	1812(2)	7217(1)	18(1)
C(6)	3874(4)	2500	7146(2)	21(1)
C(7)	1091(4)	-1088(3)	7635(2)	35(1)
C(8)	1405(3)	-1126(2)	6541(2)	26(1)
C(9)	1044(5)	-2500	7589(2)	28(1)
C(10)	1100(3)	-1816(2)	7341(2)	27(1)
C(11)	1189(3)	-1820(2)	6834(2)	25(1)
C(12)	1196(4)	-2500	6583(2)	26(1)
C(13)	1424(5)	1124(3)	5873(2)	51(2)
C(14)	100(5)	1121(4)	4987(3)	63(2)
C(15)	1404(5)	2500	5813(3)	36(2)
C(16)	1088(4)	1824(3)	5631(2)	34(1)
C(17)	445(4)	1820(3)	5246(2)	41(1)
C(18)	138(6)	2500	5063(3)	48(2)
C(19)	3307(3)	-201(3)	5578(2)	28(1)
C(20)	5253(4)	-287(3)	6046(2)	34(1)
C(21)	4146(3)	-33(3)	4781(2)	35(1)
C(22)	4198(3)	-121(3)	5287(2)	25(1)
C(23)	5076(3)	-100(3)	5508(2)	34(1)
O(1)	1774(2)	942(2)	7909(1)	31(1)
O(2)	1570(2)	788(2)	7114(1)	35(1)
O(3)	3545(2)	510(2)	6990(1)	29(1)
O(4)	4823(2)	1111(2)	7209(1)	29(1)
O(5)	439(3)	-639(2)	7563(1)	37(1)
O(6)	1733(4)	-980(3)	7932(2)	67(1)
O(7)	1905(2)	-652(2)	6750(1)	33(1)
O(8)	1110(3)	-1100(2)	6109(1)	43(1)

O(9)	2159(4)	1171(3)	6114(2)	64(1)
O(10)	864(7)	522(5)	5705(5)	49(3)
O(10')	1050(7)	556(5)	5964(4)	41(2)
O(11)	510(9)	860(7)	4643(5)	85(3)
O(11')	767(6)	543(4)	4958(3)	47(2)
O(12)	-733(3)	1067(2)	4942(2)	65(1)
O(13)	3348(2)	-122(2)	6026(1)	41(1)
O(14)	2578(2)	-323(2)	5333(1)	49(1)
O(15)	5189(3)	-944(2)	6184(2)	60(1)
O(16)	5513(3)	245(2)	6304(1)	39(1)
2				
Zn(1)	9995(1)	3067(1)	657(1)	16(1)
Zn(2)	11250	3742(1)	1250	16(1)
C(1)	7231(1)	3336(1)	606(1)	18(1)
C(2)	7391(1)	2890(1)	309(1)	16(1)
C(3)	8044(1)	2696(1)	251(1)	17(1)
C(4)	8638(1)	2863(1)	537(1)	23(1)
C(5)	8143(1)	2310(1)	-58(1)	18(1)
C(6)	12194(1)	3004(1)	855(1)	21(1)
C(7)	12334(1)	2731(1)	412(1)	22(1)
C(8)	11855(1)	2712(1)	59(1)	24(1)
C(9)	12032(1)	2484(1)	-349(1)	26(1)
C(10)	11144(2)	2917(2)	114(1)	39(1)
O(1)	7574(1)	3714(1)	550(1)	33(1)
O(2)	6730(1)	3284(1)	866(1)	30(1)
O(3)	8548(1)	2984(1)	934(1)	52(1)
O(4)	9205(1)	2836(1)	334(1)	32(1)
O(5)	12472(1)	2839(1)	1202(1)	36(1)
O(6)	11820(1)	3378(1)	831(1)	37(1)
O(7)	11002(10)	3295(6)	-135(8)	63(4)
O(7')	10862(10)	3102(7)	-181(8)	78(6)
O(8)	10823(1)	2745(1)	457(1)	44(1)

Table S3. Selected bond lengths (Å) and bond angles (°) for **1** and **2**.

1				
Zn(1)-O(16)#1	1.959(3)	Zn(2)-O(13)	2.098(3)	

Zn(1)-O(5)	1.967(3)	Zn(2)-O(2)	2.128(3)
Zn(1)-O(1)	2.018(3)	Zn(3)-O(12)#2	1.923(4)
Zn(1)-O(4)#1	2.030(3)	Zn(3)-O(14)	1.948(3)
Zn(2)-O(7)	1.954(3)	Zn(3)-O(8)	1.998(3)
Zn(2)-O(9)	1.988(4)	Zn(3)-O(10')	2.088(9)
Zn(2)-O(3)	1.992(3)		
O(16)#1-Zn(1)-O(5)	124.05(14)	O(3)-Zn(2)-O(13)	89.11(13)
O(16)#1-Zn(1)-O(1)	100.72(14)	O(7)-Zn(2)-O(2)	86.03(13)
O(5)-Zn(1)-O(1)	124.38(14)	O(9)-Zn(2)-O(2)	90.75(16)
O(16)#1-Zn(1)-O(4)#1	100.62(14)	O(3)-Zn(2)-O(2)	88.80(13)
O(5)-Zn(1)-O(4)#1	110.92(15)	O(13)-Zn(2)-O(2)	177.66(14)
O(1)-Zn(1)-O(4)#1	88.36(12)	O(12)#2-Zn(3)-O(14)	103.6(2)
O(7)-Zn(2)-O(9)	138.99(19)	O(12)#2-Zn(3)-O(8)	95.88(17)
O(7)-Zn(2)-O(3)	107.94(14)	O(12)#2-Zn(3)-O(10')	144.6(3)
O(9)-Zn(2)-O(3)	112.85(19)	O(14)-Zn(3)-O(10')	104.2(3)
O(7)-Zn(2)-O(13)	95.60(15)	O(8)-Zn(3)-O(10')	93.2(3)
O(9)-Zn(2)-O(13)	89.11(17)		

Symmetry transformations used to generate equivalent atoms: #1 $x-1/2, y, -z+3/2$; #2 $-x, -y, -z+1$.

2

Zn(1)-O(4)	1.9265(18)	Zn(1)-O(5)#2	1.9714(19)
Zn(1)-O(8)	1.939(2)	Zn(2)-O(6)	1.9293(19)
Zn(1)-O(1)#1	1.960(2)	Zn(2)-O(2)#1	1.9424(18)
O(4)-Zn(1)-O(8)	113.03(10)	O(1)#1-Zn(1)-O(5)#2	117.41(10)
O(4)-Zn(1)-O(1)#1	100.53(9)	O(6)#2-Zn(2)-O(6)	118.98(14)
O(8)-Zn(1)-O(1)#1	116.72(10)	O(6)-Zn(2)-O(2)#3	114.47(9)
O(4)-Zn(1)-O(5)#2	113.04(9)	O(6)-Zn(2)-O(2)#1	104.49(9)
O(8)-Zn(1)-O(5)#2	96.91(10)	O(2)#3-Zn(2)-O(2)#1	98.26(12)

Symmetry transformations used to generate equivalent atoms: #1 $-x+7/4, -y+3/4, z$; #2 $-x+9/4, y, -z+1/4$; #3 $x+1/2, -y+3/4, -z+1/4$.

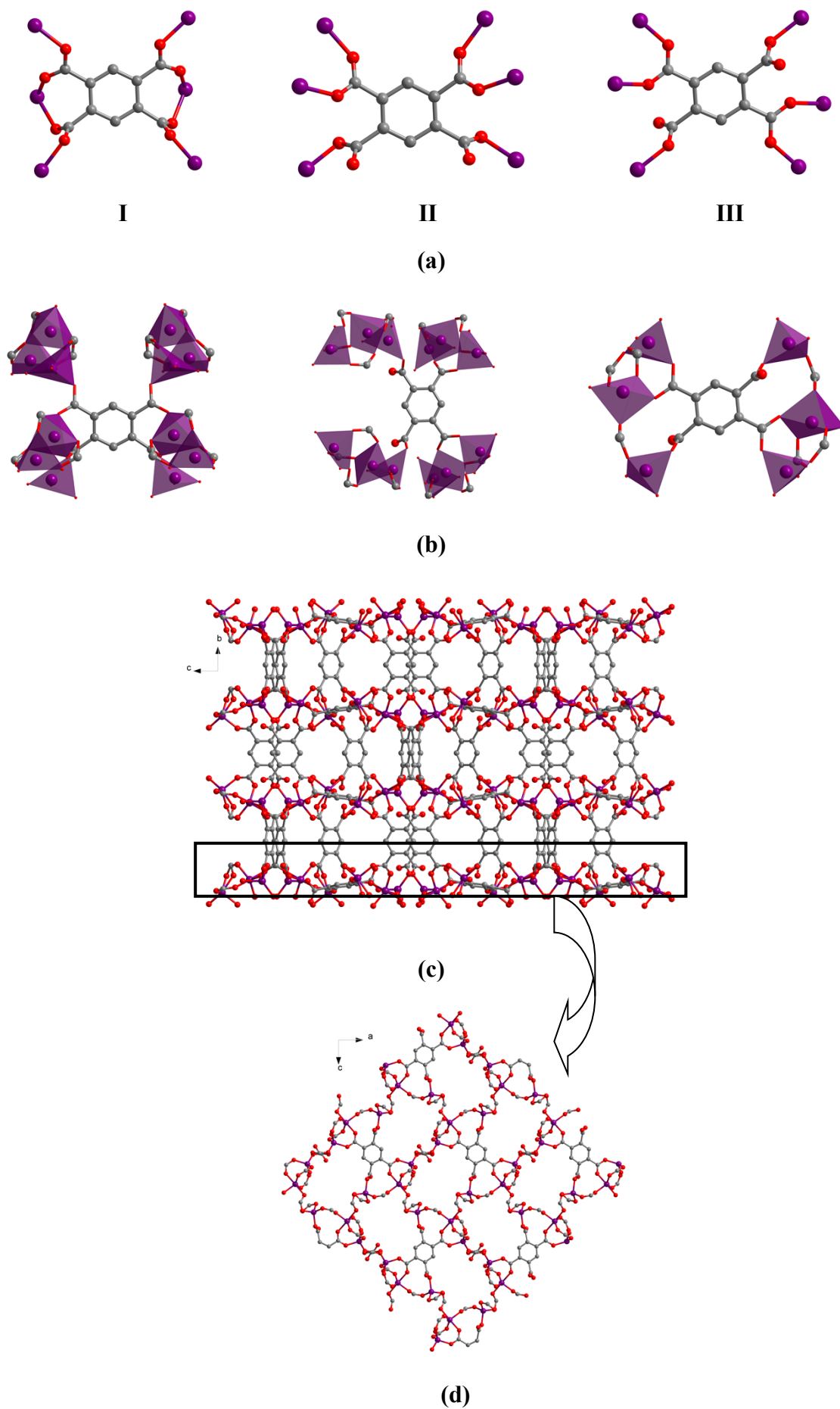
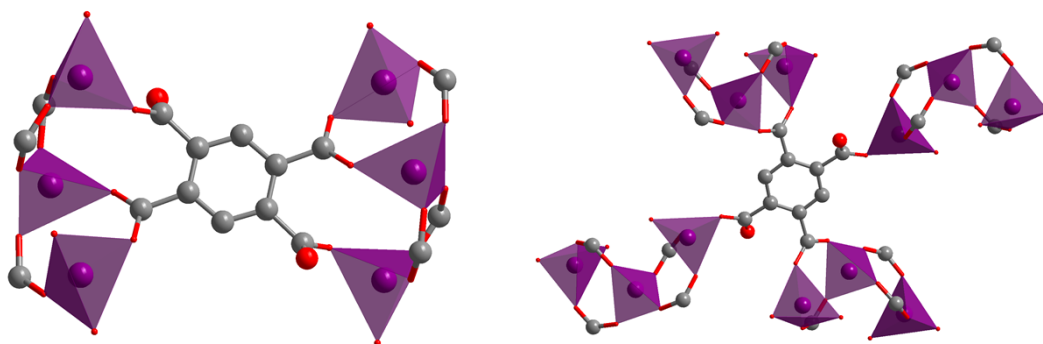
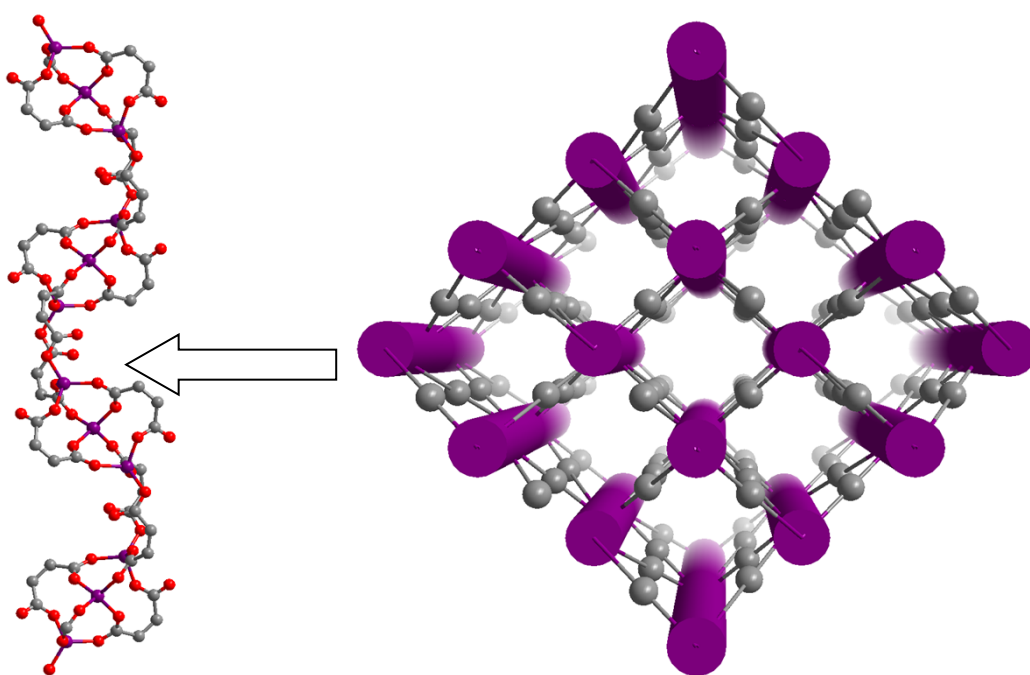


Fig. S1 (a) Three types of μ_6 -bridging modes observed in **1**; (b) The linkage between 1,2,4,5-BTC

ligands and Zn₃ trinuclear motifs; (c) The pillar-layer structure of **1** viewed from the *a*-axis direction; (d) The 2D layer in the *a,c*-plane generated by the centrosymmetric 1,2,4,5-BTC ligands.

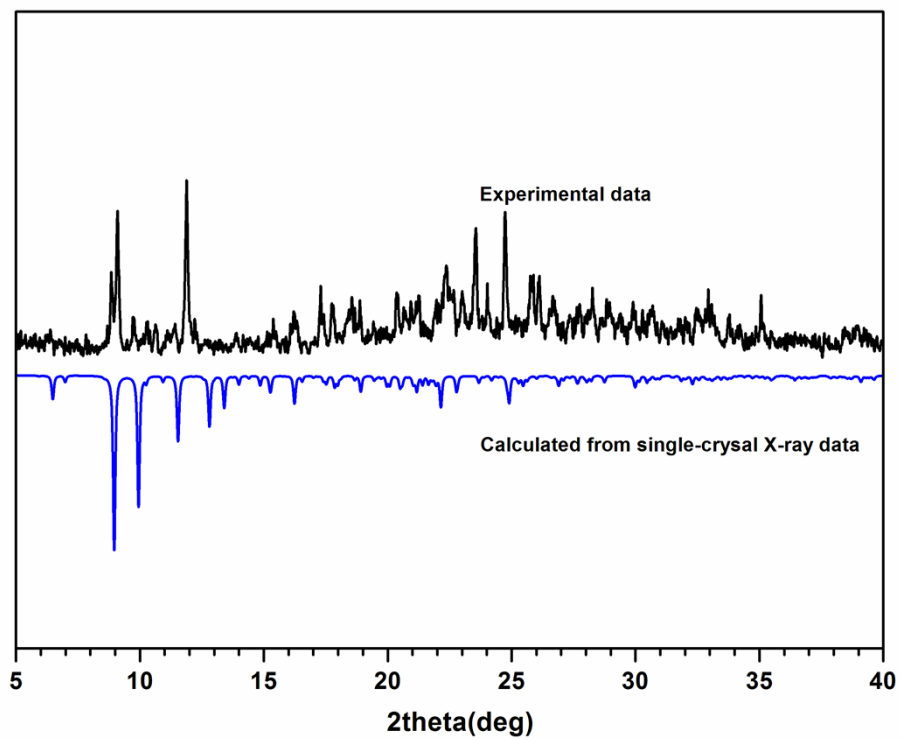


(a)

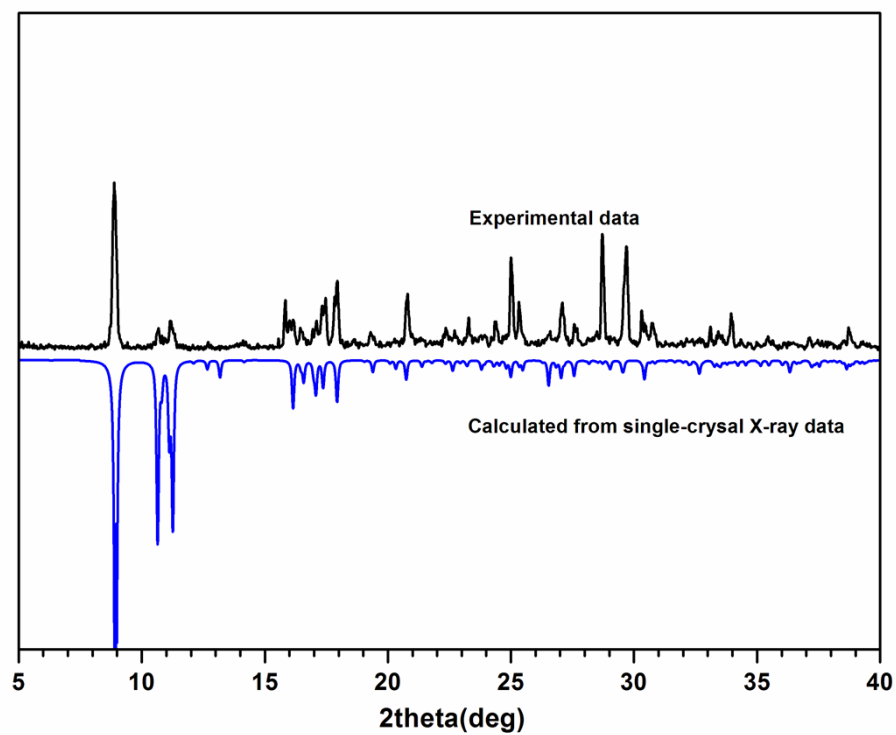


(b)

Fig. S2 (a) The linkage between 1,2,4,5-BTC ligands and Zn₃ trinuclear motifs in **2**; (b) The 1D *S*-shaped chain along the *a*-axis direction generated by the Zn₃ trinuclear subunits (left) and a schematic drawing of the rod-packing net of **2** (right).

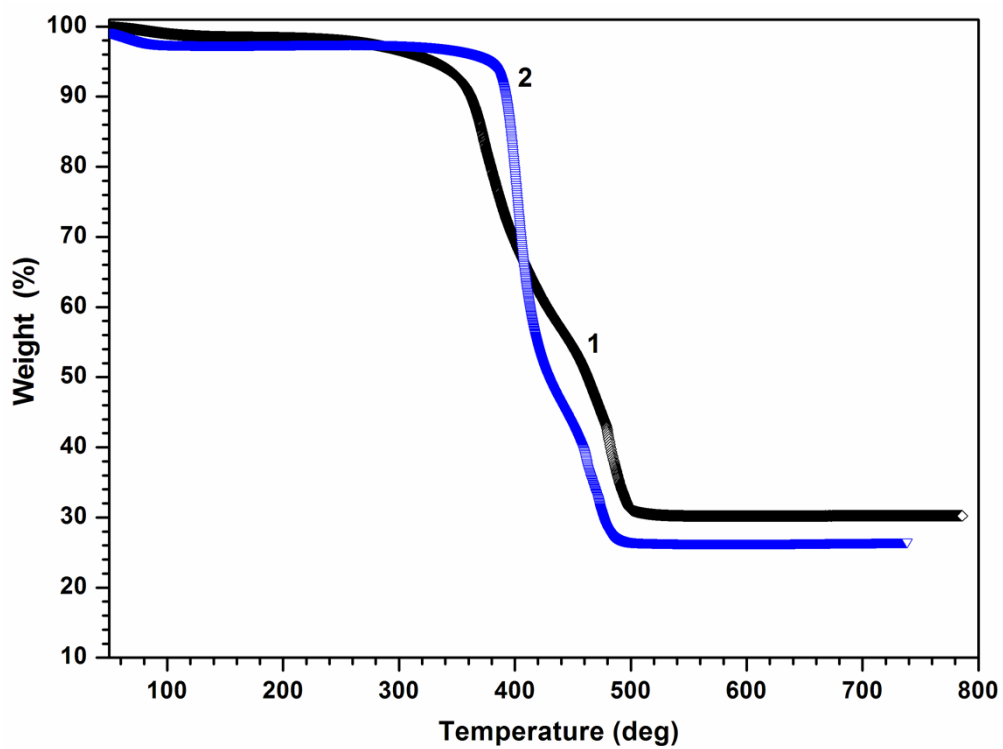


(a)

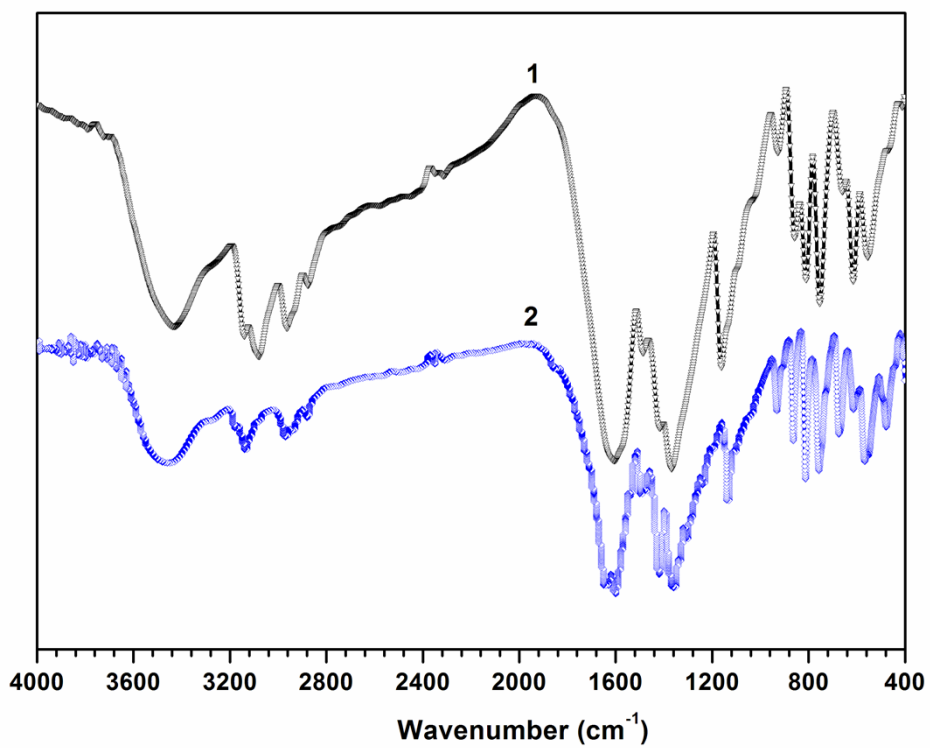


(b)

Fig. S3 X-ray powder diffraction patterns for **1** (a) and **2** (b).



(a)



(b)

Fig. S4 TGA curves (a) and FT-IR spectra (b) for 1 and 2.

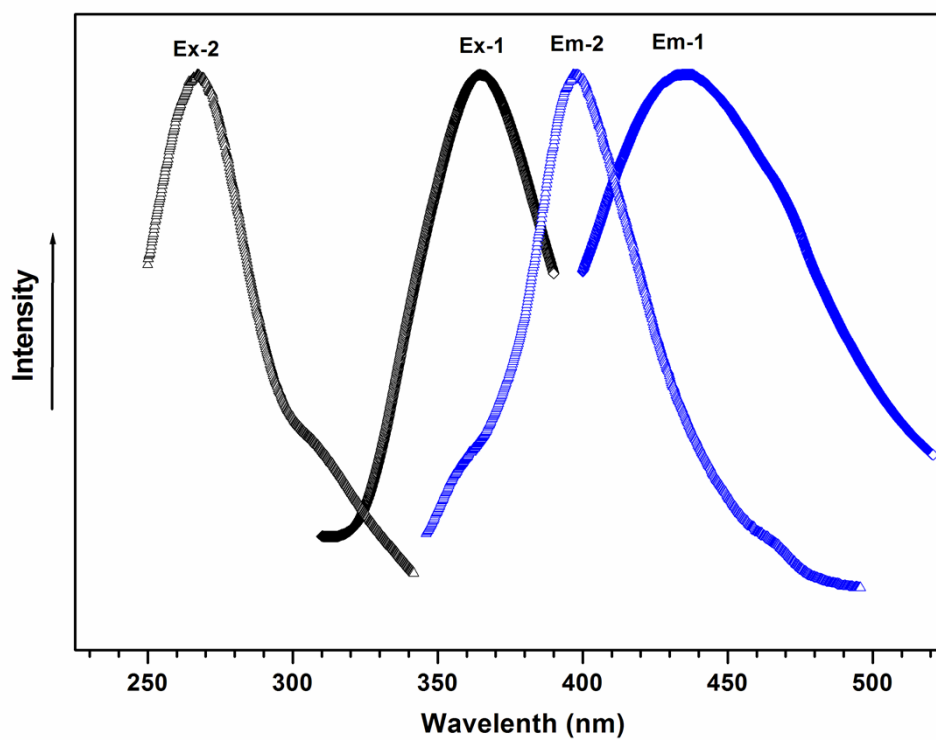


Fig. S5 Solid-state photoluminescence spectra for **1** and **2**.

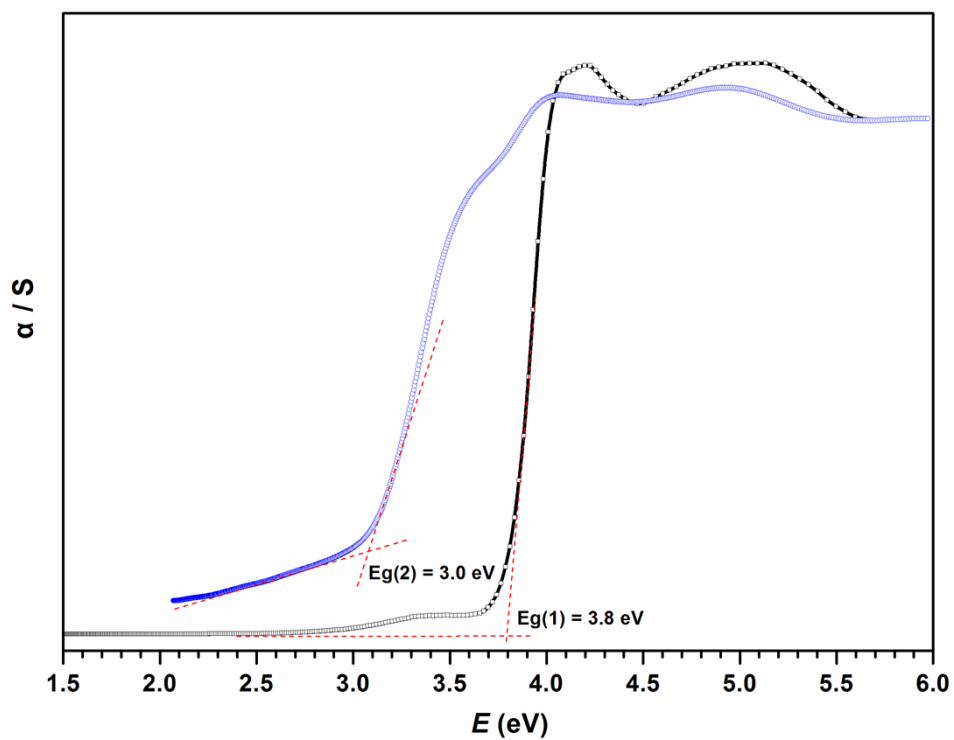
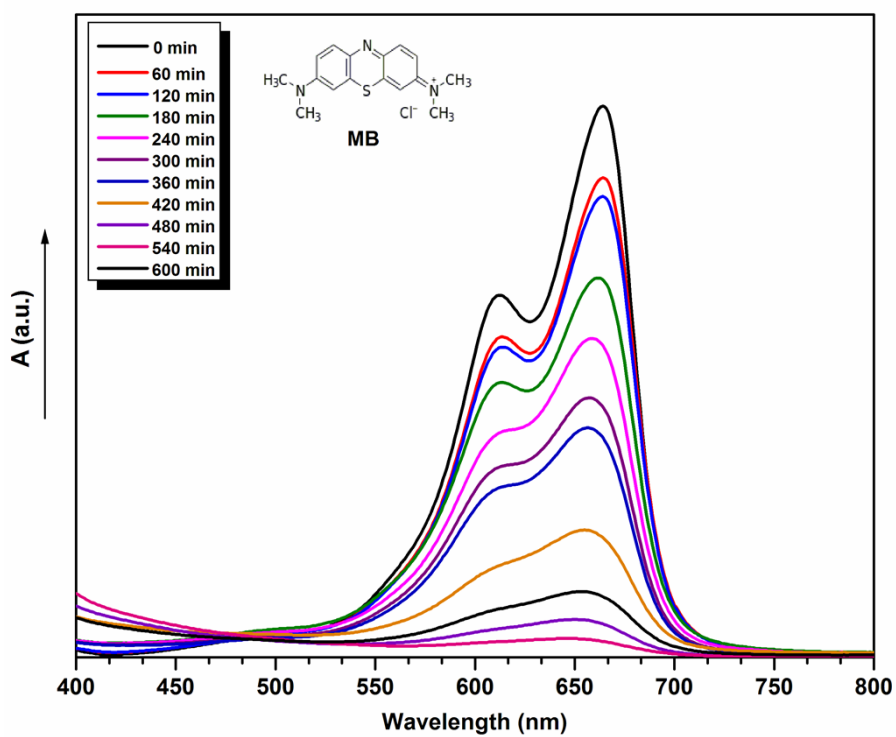
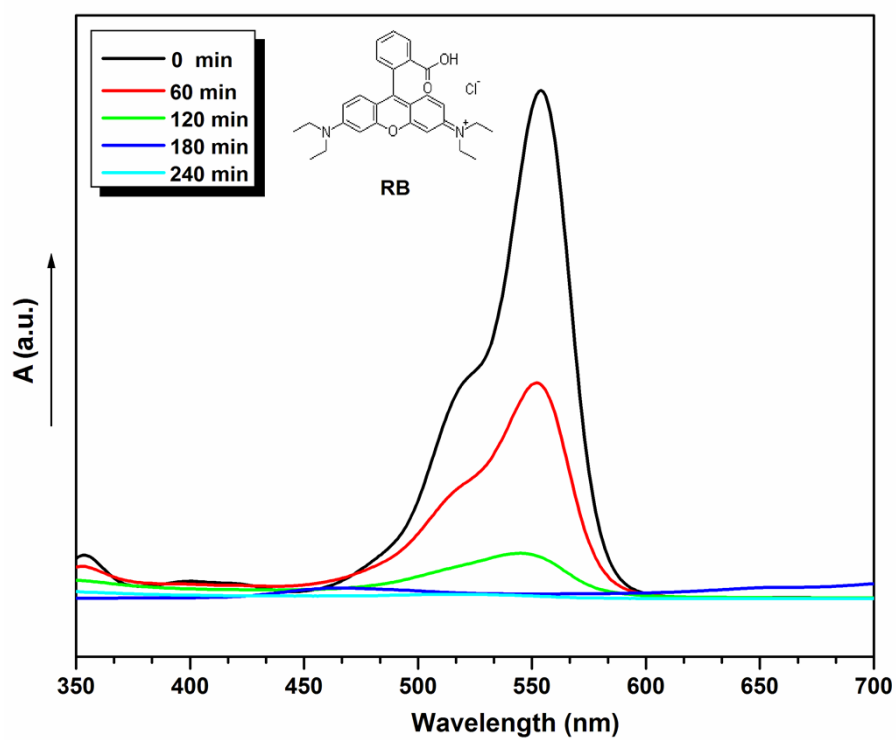


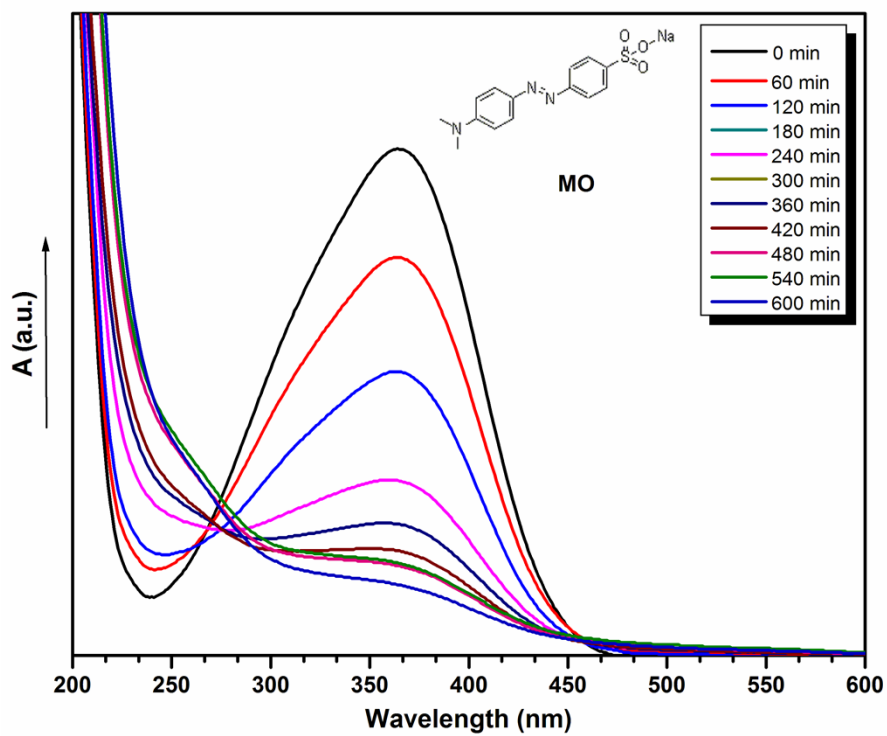
Fig. S6 Diffuse reflection spectra for **1** and **2**.



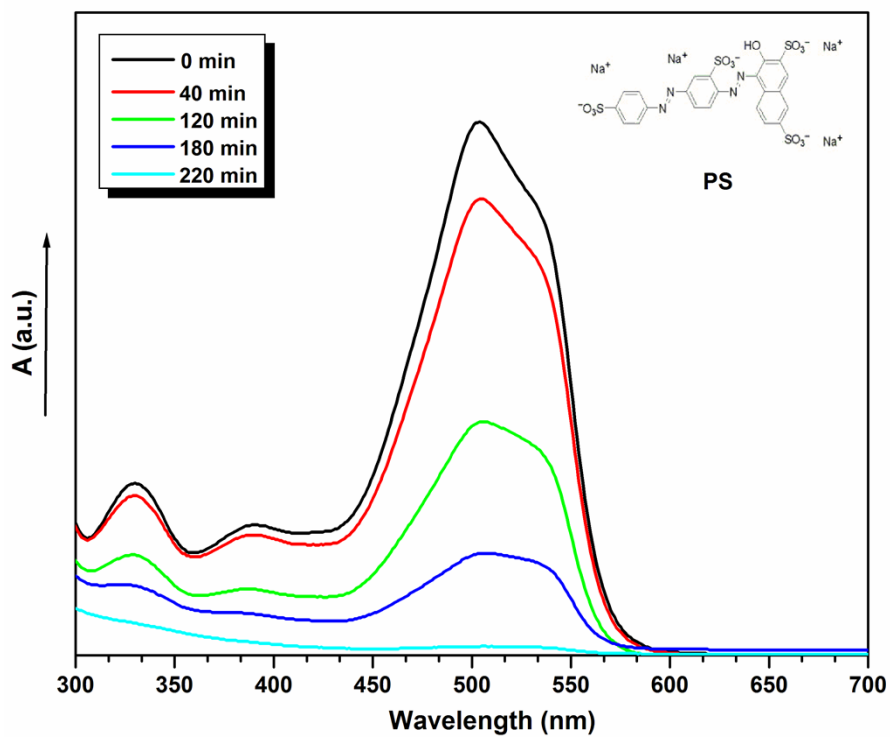
(a)



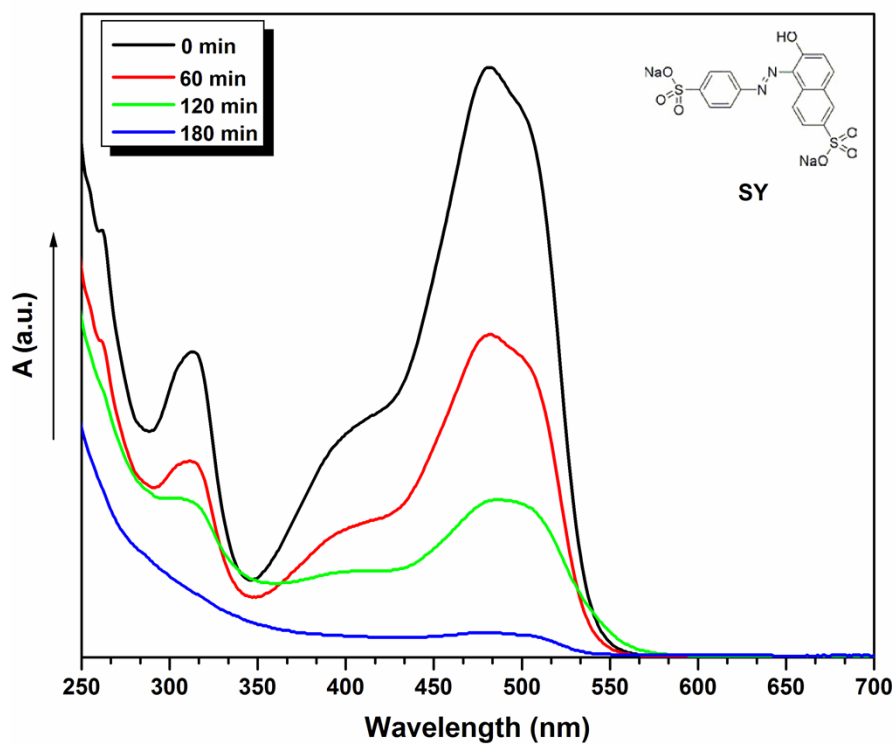
(b)



(c)



(d)



(e)

Fig. S7 The UV-Vis absorption spectra of organic dyes in water with addition of compound **1** as photocatalyst under visible-light irradiation.